SMiRT-12 / K. Kussmaul (Editor)

K23/4

ANALYTICAL STUDY ON ULTIMATE RESPONSE CHARACTERISTICS OF BASE ISOLATED STRUCTURE

K. Ishida[1], S. Yabana[1], G. Yoneda[2], J. Suhara[3] and K. Yoshikawa[4]

[1]Central Research Institute of Electric Power Industry, Chiba, Japan
[2]Takenaka Corp., Tokyo, Japan, [3]Shimizu Corp., Tokyo, Japan
[4]Kajima Corp., Tokyo, Japan

1. Introduction

In order to make sure of aseismic safety on a base-isolated reactor building, it is important to understand its earthquake response properties not only at the design level, but also at the ultimate state. From this point of view, a shaking table test was conducted to investigate the rupturing characteristics of a laminated rubber bearing and the ultimate response properties of a superstructure. This paper reports the results of a simulation analysis of its shaking table test. The restoring force loops of the rubber bearing were modeled by three different methods; a multi linear model, a smooth function model, and a rate model. It was found that the results of the shaking table test could be simulated quite accurately by any of these analytical models.

2. Outline of the Shaking Table Test

Table 1 shows the similarity law adopted in the test. The acceleration and the stress are equal to those of the prototype. The scale ratio is 1/15. Fig.1 illustrates the shape and the dimensions of the test specimen. The superstructure is a reinforced concrete rigid body with a weight of 17.8 tons. It is supported by 8 sets of lead rubber bearings(LRBs) . The LRB is a 1/15 reduced-scale model of the actual LRB for which the rated design load is 500 tons. The rubber sheet is affixed to the upper and lower flanges. Fig.2 shows the dimensions of an LRB. As an input motion, tentative design seismic motion,S1, is employed. In the tests, the input seismic motion is reduced in time to $1/\sqrt{15}$ according to the similarity law. Excitations are given repeatedly by gradually increasing the acceleration of input seismic motion by approximately 0.25 S1 each time, starting from 1.0 S1 level. Measurements were taken for the following three items. ① Shear and axial forces acting on LRBs ② Horizontal and vertical relative displacements between the shaking table and the superstructure ③ Absolute accelerations of the shaking table and the test specimen. The details of the shaking table test are described in Ref.1.

3. Loading Test of a Single Bearing

Loading tests of a single bearing are carried out by using LRBs that have the same dimensions as those used in the shaking table test. Restoring force characteristics of LRBs are investigated in various stress states created by different combinations of shear and axial forces. Fig.3 shows the results of the loading test of a single bearing. The stiffness in the strain hardening region of the horizontal hysteresis loop is softened in the cyclic loading test, compared with the monotonous loading test. In addition, once an LRB experiences a large deformation, the displacement for starting of strain hardening becomes grater. Equivalent stiffness, Keq, decreases as shear strain increases, until shear strain reaches some 200%. After that, equivalent stiffness increases due to the effects of strain hardening. Shear force at zero displacement, Qd, increases as the amplitude of shear strain increases. It is, however, almost constant over the shear strain of 200%. The equivalent damping ratio, heq, decreases as the amplitude of shear strain increases, until shear strain reaches 300%. When shear strain exceeds 400%, although the area of the hysteresis loop

increases on account of the strain hardening , the equivalent damping ratio, heq, becomes stable at approximately 5%, because the equivalent stiffness, Keq, also increases. In a simulation analysis, it is important to express the above-described restoring force characteristics of an LRB in appropriate models. The details of the loading test of a single bearing are described in Ref.2.

4. Simulation Analysis

4.1 Modeling of Restoring Force Characteristics

Restoring force characteristics of an LRB are modeled by following three different methods.
Multi linear model: As shown in Fig.4, the horizontal restoring force loop is represented by a multi-linear line. It consists of the restoring force due to the effects of the rubber part, and the absolute elasto-plastic restoring force due to the effects of the lead plug. As shown in Fig.3 a), when an LRB is deformed again after experiencing a large deformation, the displacement for starting of the strain hardening becomes larger. This phenomenon is expressed by the following formula.

$$x_s' = x_s + 0.45(x_m - x_s) \quad \cdots\cdots\cdots (1)$$

In the shaking table test, excitation is given repeatedly by increasing the acceleration of input motion step by step. The maximum horizontal displacement experienced one step before is taken as the initial value of x_m. As shown in Fig.3, the values of K_1 and Q_d depend on the amplitude of the horizontal displacement. Therefore, they are determined according to the maximum horizontal displacement in the shaking table test at each excitation level. The skeleton of a vertical restoring force loop is expressed by a tri-linear line. It is linear in the compression side, but yields in the tension side at the level of $\sigma_2 = 20\ kg/cm^2$.
Smooth Function Model: As shown in Fig.5, horizontal and vertical restoring forces are approximated using a high-order function. Horizontal restoring force loop consists of the skeleton and hysteresis curves. The skeleton curve is expressed as a quadratic function on horizontal displacement, x.

$$Q_s(x) = a_0 \cdot sgn(x) + a_1 x + a_2 x^2 + a_3 x^3 + a_4 x^4 \quad \cdots\cdots\cdots (2)$$

where, when $x > 0$, $sgn(x) = 1$, and when $x < 0$, $sgn(x) = -1$

The coefficient, a_i ($i = 0 \sim 4$), is determined based on the results of the loading test of a single bearing under static cyclic loading. "a_0" represents shear force Q_d, where horizontal displacement, x, is zero. In the simulation analysis, the value of Q_d is taken as a function on the horizontal displacement amplitude. The hysteresis curve ,$Q_L(x)$, is expressed by a quadratic function on horizontal displacement, x, as is the skeleton curve.

$$Q_L(x) = b_0 \cdot sgn(x) + b_1 x + b_2 x^2 + b_3 x^3 + b_4 x^4 \quad \cdots\cdots\cdots (3)$$

The coefficient, bi, is determined in the following way. ① The hysteresis curve passes Point (0, $-Q_d$) and Point (x_m, Q_m). ② It is tangent to the skeleton curve at Point (0, $-Q_d$). ③ When the displacement is $\beta \cdot x_m$, the distance between the skeleton and hysteresis curves is r times as large as $2Q_d$. The value of r is defined as a quadratic function on horizontal displacement. The influence of cyclic loading is taken into account by shifting the skeleton curve, as shown in Fig.5 b). The vertical restoring force loop is expressed in a linear form on the compression side and as skeleton and hysteresis curves on the tension side.
Rate Model: As shown in Fig.6, characteristics of horizontal restoring force are expressed by a rate model (Ref.3), and those of vertical restoring force are represented by a non-linear elastic model. The rate model is produced based on the following principles. ① Restoring force characteristics are expressed by a skeleton curve and a hysteresis curve. ② Restoring force loop follows the skeleton curve, when horizontal displacement exceeds the maximum displacement experienced before. Otherwise, it follows the hysteresis curve. ③ The hysteresis curve is determined by the maximum displacement experienced before.
The skeleton curve Qs (x) is expressed by the following formulas.

$$Q_s(x) = K_{eq}(x_m) \cdot x \quad \cdots\cdots\cdots (4)$$

$$K_{eq}(x_m) = c_0 + c_1 x + c_2 x^2 + c_3 x^3 \quad \cdots\cdots\cdots (5)$$

The coefficient, ci, is determined from Fig.3 b). The hysteresis curve ,Q_L, is expressed by the following formulas.

$$Q_L = Q_1 + Q_2 \quad \cdots\cdots\cdots (6)$$

$$Q_1 = K_2(\alpha + (1-\alpha)(x/x_m)^6)x \quad \cdots\cdots\cdots (7)$$

$$dQ_2/dt = (K_1 - K_2)\cdot dx/dt \cdot (1 - sgn(dx/dt)\cdot(Q_2/Q_d)) \quad \cdots\cdots\cdots (8)$$

where, $K_1 = (1 - u + u/s)\cdot Keq$ $\quad K_2 = (1-u)\cdot Keq$

$u = Q_d / Q_m$ $\quad q = \pi \cdot heq/2$

"s" represents a solution of $s\cdot(e^{2/s} - 1)(e^{2/s} + 1) = (u-q)/u$

"u" and "q" are expressed by a cubic function on horizontal displacement, based on the results of the loading test of a single bearing.

4.2 Modeling of Dynamic Response Analysis

As shown in Fig.7, the superstructure is modeled by a rigid beam and a concentrated mass. LRBs are modeled as 4 axial springs and a single shear spring. The time-history waveform of acceleration recorded at the surface center of the shaking table is employed as an input motion. Simulation analyses are carried out for input levels of 1.0 S1, 3.0 S1, and 6.0 S1.

4.3. Analytical Result

Fig.8 shows the time histories for an input of 6.0 S1. Analysis is performed on the rate model. In the test, the maximum shear strain of LRBs is 560% and LRBs are just short of rupturing. As the LRB used in the test has a small diameter of 107 mm, it shows rupture shear strain of about 600 %, which is somewhat larger than that of the actual-size LRB. The time-history waveform of the acceleration at the gravity center of the superstructure and the shear force take on sinusoidal forms when input level is low. However, when input level is high, their peaks both in the test and analysis sharpen due to the effects of strain hardening. Fig.9 shows the horizontal hysteresis loops. As remarkably shown in the case of 1.0 S1, the shear force at the point where displacement is zero becomes greater, as displacement amplitude increases. Analyses on the smooth function model and the rate model reflect this tendency. For the input of 6.0 S1, all of the three models simulate a hardening phenomenon of LRBs quite well. Fig.10 shows the relation between the axial strain and the shear strain. The tensile stiffness of LRBs is significantly smaller than its compressive stiffness. Therefore, the center of rocking vibrations shifts to the edge of the test model with an increase of overturning moment. As a result, both in the test and analysis, tensile axial strain caused by up-lift of the test model increases sharply in the area where shear strain reaches the maximum. Fig.11 illustrates the relation between the axial force and the shear strain. Just around the area where shear strain reaches the maximum, compressive axial force rises drastically. This is caused by following two reasons. One is that the increasing rate of shear strain declines and, at the same time, the response acceleration increases on account of the strain hardening. The other is that only those LRBs installed at the edge of the test model are compressive due to the movement of rocking center. The axial force becomes wavy because of the up-lift and drop-down of the superstructure. The analytical results are in good agreement with the test results. Fig.12 shows the acceleration response spectrum at the gravity center. For input of 1.0 S1, it is simulated very accurately. For input of 6.0 S1, there appear some peaks in the high frequency domain , as the peak of the acceleration time history waveform sharpens due to the influence of strain hardening. Also for input of 6.0 S1, simulation analysis results reflect this tendency. As shown in Fig.13, the maximum response values calculated by each modeling method agree quite well with test results at the input level of 1.0S1 and 3.0S1. Even for input of 6.0 S1, the differences are within a range of some 20%.

5. Conclusion

A simulation analysis was carried out on a shaking table test on a base-isolated reactor building model. Characteristics of restoring force of LRBs were expressed in three different models. It was found that the results of a shaking table test from the design level to the ultimate level could be simulated accurately by any of these models. Therefore, these analysis techniques would be very effective in evaluating aseismic safety margin of base-isolated reactor buildings.

Acknowledgement : This study was carried out as a part of the project of the Ministry of International Trade and Industry titled "Verification Tests of Fast Breeder Reactor Technology", which has been conducted since 1987.

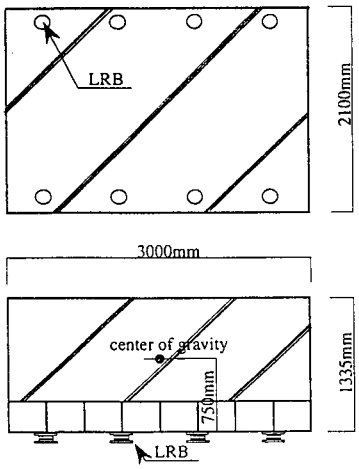

Fig.1 Shape and dimensions of superstructure

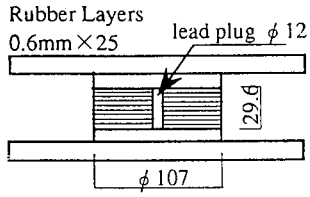

Fig.2 Lead rubber bearing

Table 1 Similutude

Scale of		Similitude
Length	L	$L_p/L_m=\lambda=15$
Acceleration	α	$\alpha_p/\alpha_m=1$
Frequency	f	$f_p/f_m=1/\sqrt{\lambda}=0.258$
Stress	σ	$\sigma_p/\sigma_m=1$
Strain	γ	$\gamma_p/\gamma_m=1$
Force	F	$F_p/F_m=\lambda^2=225$

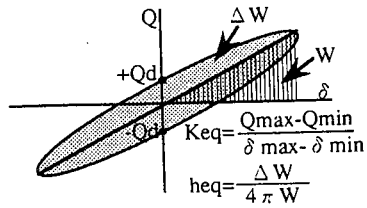

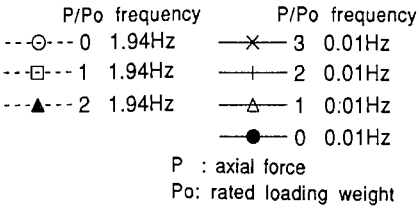

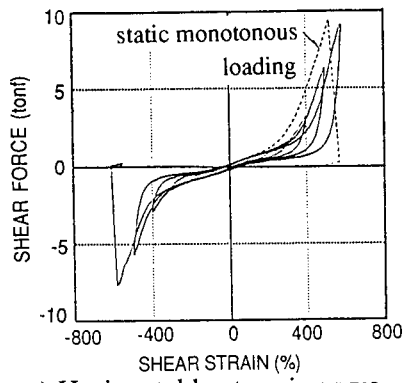

a) Horizontal hysteresis curve

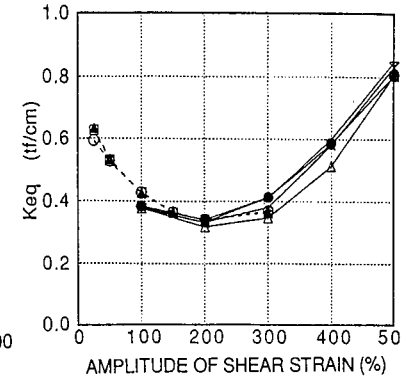

b) Equivalent stiffness Keq

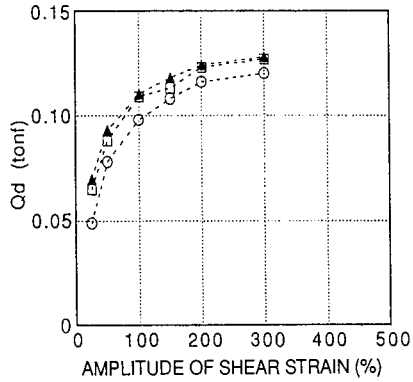

c) Shear force at 0 disp. Qd

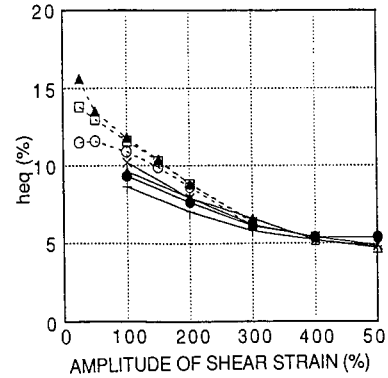

d) Equivalent damping ratio heq

Fig.3 Loading test results of a single bearing

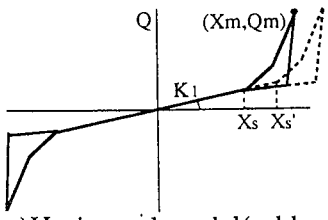

a)Horizontal model(rubber)

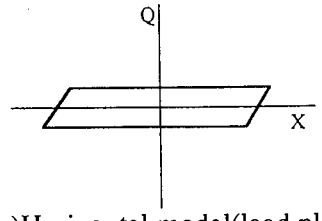

b)Horizontal model(lead plug)

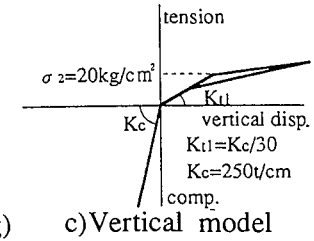

c)Vertical model

Fig.4 Restoring force loop by multi linear model

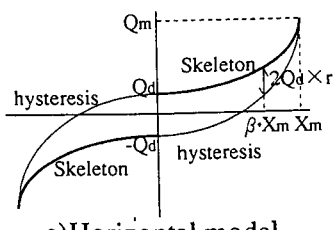

a)Horizontal model

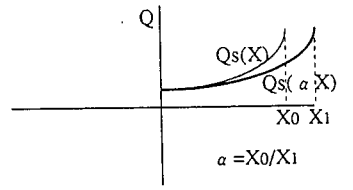

b)Evaluation of dependence on iterative deformation

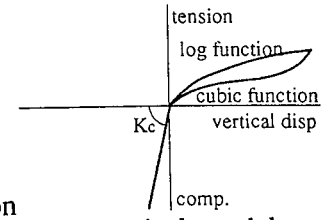

c)Vertical model

Fig.5 Restoring force loop by smooth function model

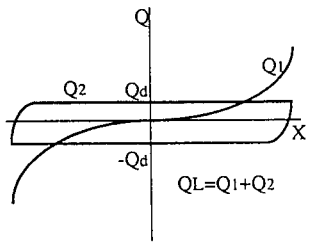

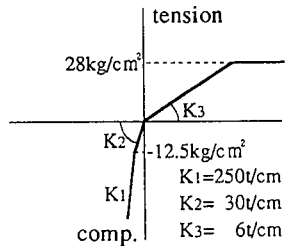

a)Horizontal model(hysteresis) b)Vertical model

Fig.6 Restoring force loop by rate model

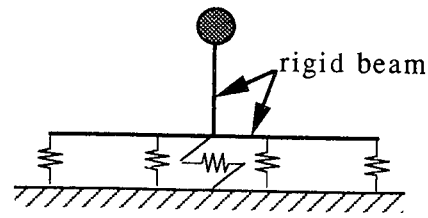

Fig. 7 Simulation analysis model

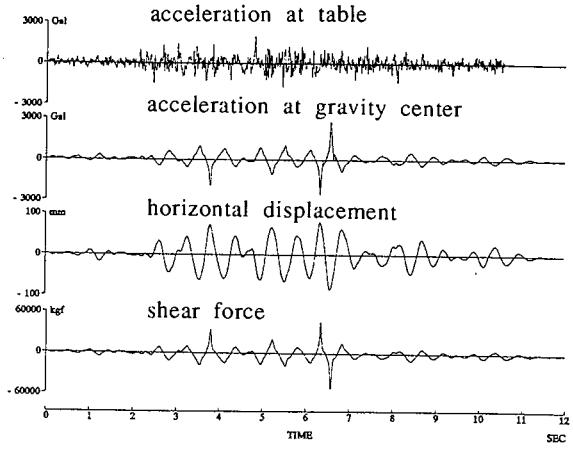

a) Experiment

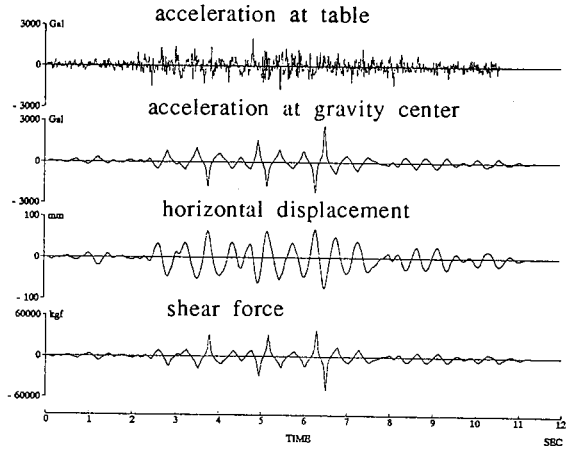

b) Analysis by rate model

Fig.8 Time histories at 6.0S1

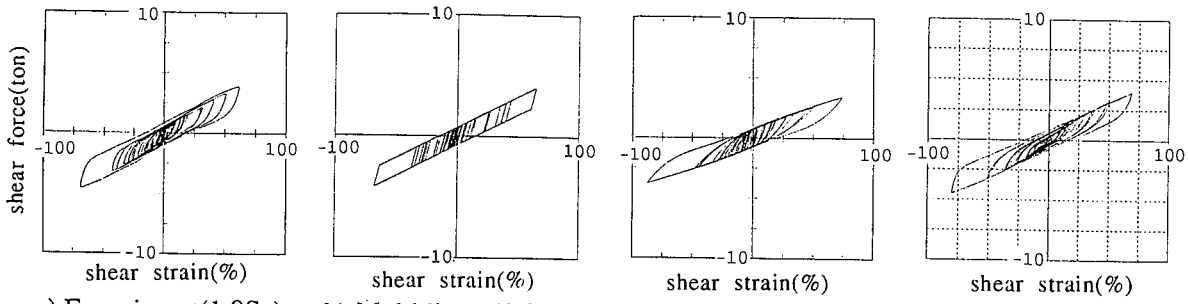

a) Experiment(1.0S1) b) Multi linear(1.0S1) c)Smooth function(1.0S1) d)Rate model(1.0S1)

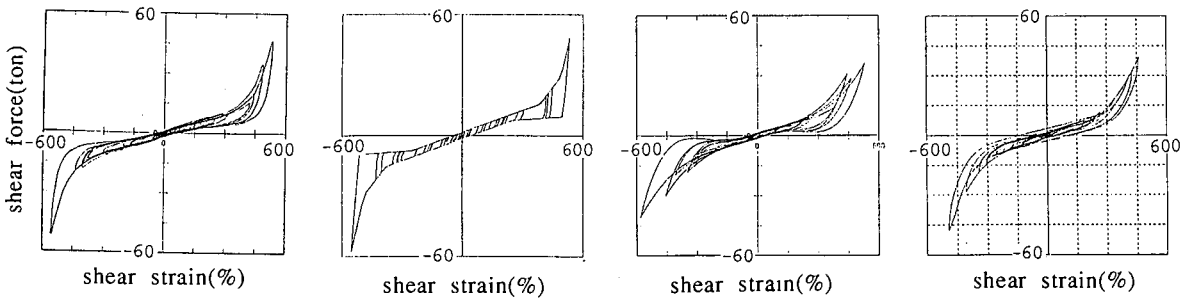

e) Experiment(6.0S1) f) Multi linear(6.0S1) g)Smooth function(6.0S1) h)Rate model(6.0S1)

Fig.9 Relationship between shear force and shear strain

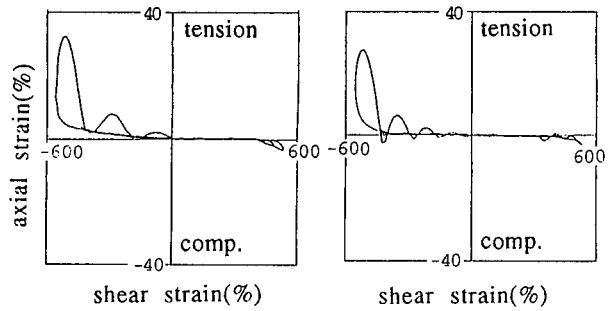

Fig. 10 Relationship between axial strain and shear strain (Multi linear model, 6.0S1)

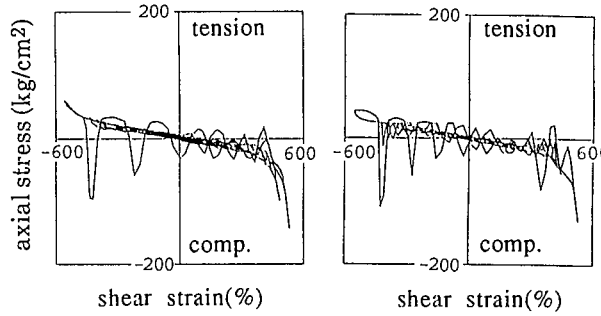

Fig. 11 Relationship between axial force and shear strain (Multi linear model, 6.0S1)

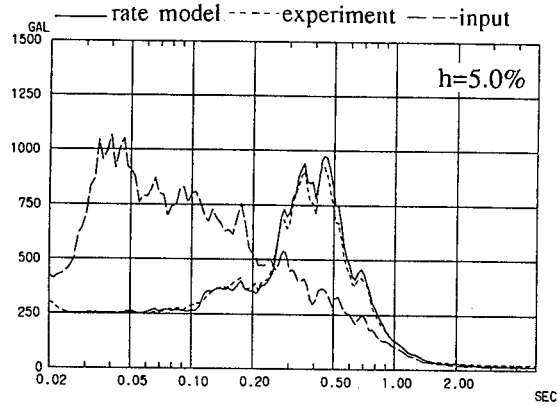

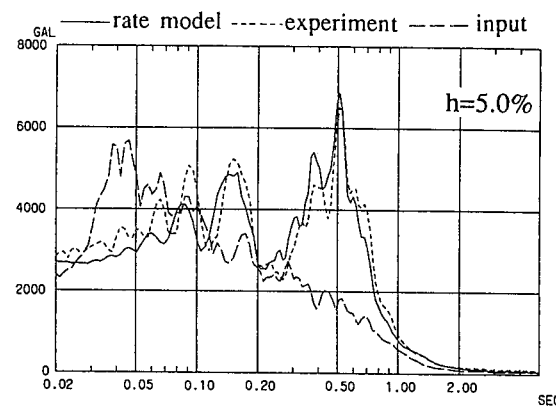

Fig. 12 Response spectra at the center of gravity

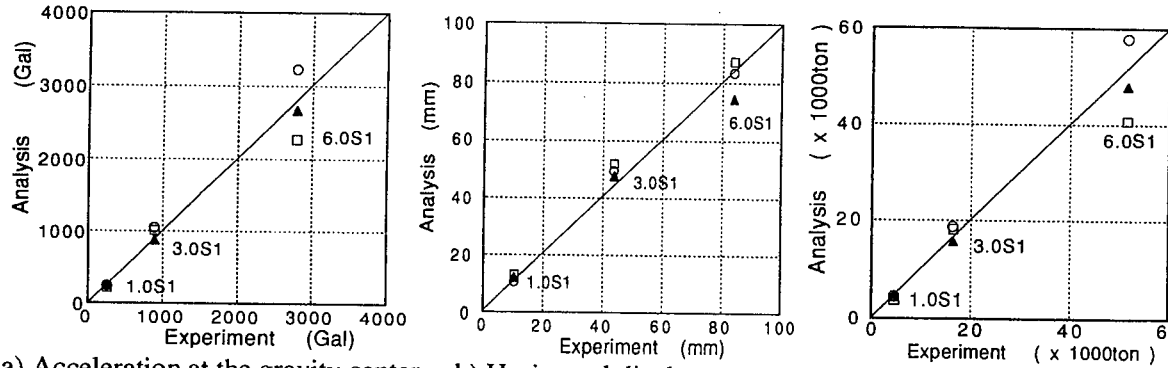

Fig. 13 Comparison between maximum response values of experiment and those of analysis

References
1) Ishida, K., Moteki, M., Yoneda, G., et al., 1992, Shaking table test on ultimate behavior of seismic isolation system Part 1 & 2, 10th WCEE,vol.4, pp2271～2276, pp2411～2416
2) Ishida, K., Iizuka, M., et al., 1991, Failure tests of laminated rubber bearings, 11th SMIRT, vol.K2, pp241～246
3) Fujita, T., Suzuki, S., et al., 1991, Ultimate Strength of Seismic Isolation System Using High Damping Rubber Bearings for Buildings, trans. Jpn. Soc. Mech. Eng., Vol.57, No.544, C